JOURNAL OF BACTERIOLOGY, Apr. 1990, p. 2141–2149
0021-9193/90/042141-09$02.00/0

Vol. 172, No. 4

Evaluation of Freeze-Substitution and Conventional Embedding Protocols for Routine Electron Microscopic Processing of Eubacteria

LORI L. GRAHAM* AND T. J. BEVERIDGE

Department of Microbiology, College of Biological Sciences, University of Guelph, Guelph, Ontario, Canada N1G 2W1

Received 25 August 1989/Accepted 5 January 1990

Freeze-substitution and more conventional embedding protocols were evaluated for their accurate preservation of eubacterial ultrastructure. Radioisotopes were specifically incorporated into the RNA, DNA, peptidoglycan, and lipopolysaccharide of two isogenic derivatives of *Escherichia coli* K-12 as representative gram-negative eubacteria and into the RNA and peptidoglycan of *Bacillus subtilis* strains 168 and W23 as representative gram-positive eubacteria. Radiolabeled bacteria were processed for electron microscopy by conventional methods with glutaraldehyde fixation, osmium tetroxide postfixation, dehydration in either a graded acetone or ethanol series, and infiltration in either Spurr or Epon 812 resin. A second set of cells were simultaneously freeze-substituted by plunge-freezing in liquid propane, substituting in anhydrous acetone containing 2% (wt/vol) osmium tetroxide, and 2% (wt/vol) uranyl acetate, and infiltrating in Epon 812. Extraction of radiolabeled cell components was monitored by liquid scintillation counting at all stages of processing to indicate retention of cell labels. Electron microscopy was also used to visually confirm ultrastructural integrity. Radiolabeled nucleic acids and wall components were extracted by both methods. In conventionally embedded specimens, dehydration was particularly damaging, with ethanol-dehydrated cells losing significantly more radiolabeled material during dehydration and subsequent infiltration than acetone-treated cells. For freeze-substituted specimens, postsubstitution washes in acetone were the most deleterious step for gram-negative cells, while infiltration was more damaging for gram-positive cells. Autoradiographs of specimens collected during freeze-substitution were scanned with an optical densitometer to provide an indication of freezing damage; the majority of label lost from freeze-substituted cells was a result of poor freezing to approximately one-half of the cell population, thus accounting for the relatively high levels of radiolabel detected in the processing fluids. These experiments revealed that gram-positive and gram-negative cells respond differently to freezing; these differences are discussed with reference to wall structure. It was apparent that the cells frozen first (i.e., the first to contact the cryogen) retained the highest percentage of all radioisotopes, and the highest level of cellular infrastructure, indicative of better preservation. The preservation of these select cells was far superior to that obtained by more conventional techniques.

Although freeze-substitution yields images which are strikingly different from those obtained by more conventional techniques and which have profoundly affected current views of bacterial ultrastructure and the native distribution of cellular constituents (11), freeze-substitution has been used only infrequently in the study of procaryotic structure. Several factors are responsible for the limited use of freeze-substitution. The technique requires expertise in ultrarapid freezing, the necessary equipment is frequently expensive, and more importantly, there is no easy way to determine how well the cells have been preserved. Our study uses a relatively inexpensive, laboratory-built freezing apparatus which relies on rapid immersion (greater than 5 m/s) of the specimen into −196°C liquid propane (freeze-plunging). Selective incorporation of isotopes into distinct structures of *Escherichia coli* and *Bacillus subtilis*, as representative gram-negative and -positive eubacteria, respectively, has made it possible to monitor both freezing damage and retention of cellular constituents during all steps of the freeze-substitution protocol. At the same time, it has allowed freeze-substitution to be compared with a more conventional embedding regimen.

Systematic investigation of the effects of processing protocols on samples for electron microscopy has been limited. Investigations into the conventional processing of mammalian (5, 6) and plant (4) tissues have shown that the type of fixative, dehydrating agent, and resin as well as the duration of incubation in each affects the degree of extraction of cellular constituents. Variations in fixation regimens have also been reported to dramatically alter the appearance of procaryotes (1, 7, 15).

The most exhaustive study to date relied on extraction of lipids from *Acholeplasma laidlawii*, an atypical bacterium that lacks a cell wall. The results of experiments evaluating the degrading effects of routine embedding (18), low-temperature embedding (17), and freeze-substitution (19) suggest that at least with this bacterium, rapid freezing and substitution is the best method of preservation.

Our study represents the first attempt to examine retention of both wall and cytoplasmic components from gram-positive and gram-negative eubacteria during simultaneous processing for freeze-substitution and conventional embedding. In an accompanying manuscript (8), we show that although several fixatives may be used for the freeze-substitution process, osmium tetroxide and uranyl acetate in anhydrous acetone yield superior results as measured both visually by electron microscopy and by radiolabeling.

(A portion of these data was presented previously [L. L. Graham and T. J. Beveridge, Abstr. Annu. Meet. Am. Soc. Microbiol. 1988, J4, p. 205].)

* Corresponding author.

MATERIALS AND METHODS

Bacterial strains. Both *E. coli* mutant strains were derivatives of K-12. Strain SFK11 was kindly supplied by S. F. Koval, University of Western Ontario. It is an auxotrophic mutant requiring diaminopimelic acid (DPM; Sigma Chemical Co.), galactose, and lysine for growth (3). Strain SFK11 was maintained on nutrient agar (Difco) slants supplemented with 3% (wt/vol) yeast extract (Difco), 52 μg of DPM per ml, 105 μg of DL-lysine (Sigma) per ml, and 2 mg of D-galactose (Fisher Scientific Co.) per ml.

E. coli W7 was kindly provided by J.-V. Höltje, Max Planck Institut für Virusforschung, Abteilung Biochemie, Tubingen, Federal Republic of Germany. This strain is also an auxotrophic mutant requiring DPM and lysine in the growth medium. This strain was maintained on slants composed of nutrient agar supplemented with yeast extract, DPM, and DL-lysine as outlined above.

B. subtilis W23 was kindly supplied by H. Pooley, Université de Lausanne, Lausanne, Switzerland. Strains W23 and 168 were maintained on slants of brain-heart infusion agar (Difco).

Radiolabeling of bacteria. Radiolabeling of the peptidoglycan and RNA fractions of *E. coli* SFK11 was accomplished with a 1% inoculum of an exponential-phase culture in medium consisting of (per liter) 8 g of nutrient broth, 3 g of yeast extract, and 0.05 g of lysine with 5.3 μg of DPM per ml (to force uptake of tritiated DPM, unlabeled DPM was used at 1/10 the required concentration in labeling medium) and 2 mg of galactose per ml. Cells were grown for 6 h at 37°C and 150 rpm (OD_{600}, 0.13), labeled by the addition of 25 μCi of [^{3}H]DPM (DL-*meso*-2,6-diamino[G-^{3}H]pimelic acid dihydrochloride; specific activity, 1 Ci/mmol; Amersham Corp.) and 2.5 μCi of [2-^{14}C]uracil (specific activity, 54 mCi/mmol; Amersham) and incubated for an additional 7 h (OD_{600}, 1.23). Labeling of the lipopolysaccharide (LPS) and DNA fractions of this strain was accomplished in the same medium containing 53 μg of DPM per ml in the absence of galactose. To obtain maximum incorporation of labeled galactose into the LPS component, 10 μCi of D-[1-^{14}C]-galactose (specific activity, 61 mCi/mmol; Amersham) was added at inoculation, and cells were grown for 6 h (OD_{600}, 0.13) as described above, at which time 25 μCi of [5-^{3}H]thymidine (specific activity, 14.2 Ci/mmol; Amersham) was added, and cells were incubated for an additional 7 h (OD_{600}, 1.23).

The peptidoglycan and RNA fractions of *E. coli* W7 were labeled in the same medium containing 6.4 μg of DPM per ml. After 3 h of incubation (OD_{600}, 0.25), 25 μCi of [^{3}H]DPM and 2.5 μCi of [^{14}C]uracil were added, and cells were harvested after an additional 4 h of incubation (OD_{600}, 1.2).

Labeling of *B. subtilis* 168 and W23 was accomplished in Spizizen minimal medium (16) supplemented with 0.5% (vol/vol) glycerol (Fisher Scientific), 2 mg of *N*-acetylglucosamine (GlcNAc; ICN Pharmaceuticals) per ml, and 50 μg of tryptophan (Sigma) per ml as described by Mobley et al. (13). A 2% inoculum from an exponential-phase culture in Spizizen minimal medium containing 6 mg of GlcNAc per ml was transferred to fresh supplemented minimal medium. Cells were grown for 4 h at 37°C and 180 rpm (OD_{600}, 0.25), labeled by the addition of 25 μCi of [^{3}H]GlcNAc (*N*-acetyl-D-[1-^{3}H]glucosamine; specific activity, 1.7 Ci/mmol; Amersham) and 2.5 μCi of [^{14}C]uracil, and harvested after an additional 1.5 h of incubation (OD_{600}, 1.1).

Conventional embedding of radiolabeled bacteria. Before cells were harvested for processing, samples of all cultures were collected and the cell number was determined by OD_{600} and CFU with serial dilution and plate counts. Samples were also filtered through cellulose nitrate filters (0.45-μm pore size; Millipore) to determine label uptake, and the filtrate was retained to check for residual label.

Equal amounts of radiolabeled cells were harvested by centrifugation (6,000 × *g*, 20 min), and the resulting pellet was suspended in 4% (vol/vol) glutaraldehyde (Marivac Ltd.) in 0.05 M HEPES (*N*-2-hydroxyethylpiperazine-*N'*-2-ethanesulfonic acid; Research Organics Inc.) buffer, pH 6.8. After 2 h of fixation at room temperature, cells were pelleted, enrobed in 2% Noble agar, and cut to form blocks 3 mm in length and 1 mm in diameter. These blocks were washed five times for 15 min each in HEPES buffer, post-fixed for 2 h at room temperature in 2% (wt/vol) aqueous osmium tetroxide (Fisher), and washed in buffer an additional five times They were then dehydrated through a graded acetone or ethanol series of 30, 50, 70, 95, 100, and 100% (dehydration step), followed by a single 15-min wash in dehydrating solvent–propylene oxide (1:1) and two 10-min washes in 100% propylene oxide (transition step). After infiltration overnight at room temperature in either Spurr low-viscosity resin or Epon 812 mixed in a 1:1 ratio with propylene oxide (infiltration step), blocks were embedded in fresh resin and polymerized at 60°C for 8 h (Spurr resin) or 36 h (Epon 812 resin).

Freeze-substitution of radiolabeled bacteria. After being harvested by centrifugation, radiolabeled cells were incubated in 18% (vol/vol) glycerol (Fisher Scientific) in 0.05 M HEPES buffer, pH 6.8, for 20 min at room temperature. Although no significant difference ($P < 0.01$) was observed in the percentage of radiolabel leached from *E. coli* and *B. subtilis* cells treated with glycerol prior to freeze-substitution relative to that from untreated cells (data not shown), we have found that glycerol has protective value for bacteria such as *Vibrio*, *Campylobacter*, *Haemophilus*, and *Leptothrix* spp. and therefore included it in this protocol for routine freeze-substitution. Bacteria were pelleted in an Eppendorf centrifuge, and a volume of molten 2% (wt/vol) Noble agar (ca. 60°C) equal to the pellet was added and mixed. The suspension was immediately spread as a thin layer (ca. 20 to 30 μm as visualized by electron microscopy) on a cellulose-ester filter (Gelman Sciences) with a sterile glass microscope slide. Wedge-shaped portions of this filter were plunge-frozen (pointed sharp end first) with a device designed and built at the University of Guelph, Guelph, Ontario (L. L. Graham, E. Bullock, R. Harris, R. Humphrey, and T. J. Beveridge, unpublished data) (freezing step). Frozen samples were then transferred to glass vials containing −196°C substitution medium and physically pressed down onto the surface to ensure that the cells were in direct contact with the frozen medium. Substitution medium, prepared fresh prior to use, consisted of 2% (wt/vol) osmium tetroxide and 2% (wt/vol) uranyl acetate (Fisher Scientific) in anhydrous acetone in the presence of molecular sieve (sodium alumino silicate; pore diameter, 0.4 nm; Sigma) (8). The time elapsed between spreading on the membrane and transfer of plunge-frozen cells to substitution medium rarely exceeded 2 min. Vials were sealed and substituted at −80°C for 72 h undisturbed (substitution step). Vials were then removed, allowed to come to room temperature, and washed six times for 15 min each in fresh anhydrous acetone to remove excess fixative (acetone wash step). Samples were infiltrated overnight at room temperature in an acetone–Epon 812 mixture (1:1) (infiltration step), embedded in fresh Epon, and polymerized at 60°C for 36 h.

TABLE 1. Total percent ^3H and ^{14}C cpm detected as soluble material in processing fluids during conventional embedding of *E. coli* SFK11 and W7 and *B. subtilis* 168 and W23 with acetone and ethanol as dehydrating agents

Dehydrating agent	% of added cpm[a]									
	E. coli						*B. subtilis*			
	SFK11		SFK11		W7		168		W23	
	[^{3}H]DPM	[^{14}C]Ura	[^{3}H]Thy	[^{14}C]Gal	[^{3}H]DPM	[^{14}C]Ura	[^{3}H]GlN	[^{14}C]Ura	[^{3}H]GlN	[^{14}C]Ura
Acetone	4.85	3.93	3.82	2.52	2.3	2.65	6.47	2.64	9.56	1.94
Ethanol	4.86	4.74	5.03	3.88	2.58	3.36	6.05	2.69	7.14	2.07

[a] DPM, Diaminopimelic acid; Ura, uracil; Thy, thymidine; Gal, galactose; GlN, *N*-acetylglucosamine.

Collection of samples and solvents for liquid scintillation counting. During conventional embedding, triplicate sample blocks were collected after glutaraldehyde fixation, after osmium fixation (wash step 5), after the second wash in 100% propylene oxide, and after overnight plastic infiltration. From initial experiments, it was determined that label detection was negligible in both glutaraldehyde and osmium tetroxide fixation solutions and their subsequent washes. Therefore, these solutions were not collected or analyzed in the data presented here. All dehydrating solutions, propylene oxide washes, and infiltrating resins were retained for analysis.

For freeze-substitution, triplicate sample wedges were collected immediately before and after plunge-freezing, after substitution (but prior to washes in anhydrous acetone), and after overnight infiltration in the acetone-Epon 812 mixture. In addition, all substitution fluids, all acetone washes, and all infiltration resins were retained for analysis. Samples from conventional and freeze-substituted preparations were dissolved in 0.5 ml of Protosol (New England Nuclear Corp.) for solubilization prior to the addition of 10 ml of scintillation cocktail (toluene in the presence of Omnifluor; New England Nuclear). In the case of aqueous solvents, Scintverse (Fisher Scientific) was substituted for the toluene-based cocktail. Counting was performed on a Beckman LS-3150T liquid scintillation counter. After correction for quenching, all data are presented as the percent counts per minute (cpm) detected in samples or washes and represent the mean of three independent experiments.

Autoradiography. To monitor the extent of freezing damage, freeze-substitution wedges were collected prior to and after plunge-freezing, after substitution, and after infiltration; all wedges were mounted on clean glass slides. Slides were covered with Saran Wrap, which inhibits penetration of soft β-emitters such as ^3H but not moderate β-emitters such as ^{14}C. Autoradiographic film (Hyperfilm-^{3}H; Amersham) was placed directly against samples, and a second glass slide was placed over the film and clamped in place to ensure constant contact between the samples and the autoradiographic emulsion. The film was exposed for 18 h at room temperature and developed as directed by the supplier.

Optical densitometry. (i) Freeze-substitution wedges. A Joyce-Lobel 3CS optical densitometer (Joyce-Lobel Ltd., Gateshead, England), set at a track width of 40 μm, was used to scan autoradiograms and produce tracings of grain density.

(ii) Cell wall profiles. High-magnification negatives of bacterial cell walls were produced on high-grain-density, orthochromatic Graphic Arts film (Du Pont) from images originally obtained by electron microscopy. These negatives were also scanned perpendicular to the cell wall cross section to yield a profile of bacterial cell walls.

Electron microscopy. Bacteria prepared by the conventional embedding and freeze-substitution protocols were thin-sectioned on a Reichert-Jung Ultracut E ultramicrotome and mounted on Formvar carbon-coated copper grids. To improve contrast, some sections were poststained in 2% (wt/vol) aqueous uranyl acetate followed by lead citrate (14). Electron microscopy was performed on a Philips EM300 electron microscope at an operating voltage of 60 kV under standard operating conditions with the cold trap in place.

Statistical analyses. Two-tailed variance ratio tests (*F* value) were used to establish homogeneity in sample populations. The paired Student's *t* test was then used to compare values obtained under all labeling conditions.

RESULTS

Radiolabel retention in conventionally embedded bacteria. A total of five different dual-labeling combinations were used for examination of radiolabel retention. *E. coli* SFK11 was labeled in either the LPS and DNA fractions or the peptidoglycan and RNA fractions, strain W7 was labeled in the peptidoglycan and RNA fractions, and *B. subtilis* strains 168 and W23 were both labeled in their peptidoglycan and RNA fractions. Unfortunately, we were unable to use cellulose-ester membranes (as used for freeze-substituted samples) for the conventional embedding because the membrane disintegrated during processing or the entire cell-agar layer detached from the membrane. In both cases, the residual agar-bacteria material was very fragile and difficult to keep intact during subsequent processing stages.

Table 1 lists the total percent cpm detected in processing fluids when bacteria were treated by conventional means with acetone or ethanol as the dehydrating agent. Generally, higher levels of radiolabel were leached from cells when dehydration was performed in ethanol ($P < 0.002$). The use of acetone, however, resulted in a greater amount of soluble peptidoglycan from *B. subtilis* 168 and W23, yet extraction of the RNA label from these cells was greater in ethanol-treated cells.

Each of the three stages of conventional preparation subsequent to fixation and postfixation was associated with cell damage (Fig. 1). The dehydration step was particularly damaging; usually ethanol solubilized more of the labeled material than acetone. No correlation was found between the concentration of dehydrating agent and the degree of solubilization; the degree of leaching remained constant. The transition step through propylene oxide also caused leaching of labeled material. This was especially true for the first solution change (propylene oxide–dehydrating agent in a 1:1 ratio), in which label loss exceeded that during the subsequent two changes in 100% propylene oxide. Leaching was observed to be greater in cells that were first dehydrated in ethanol. Although propylene oxide is generally used as a transition solvent between the dehydration and embedding

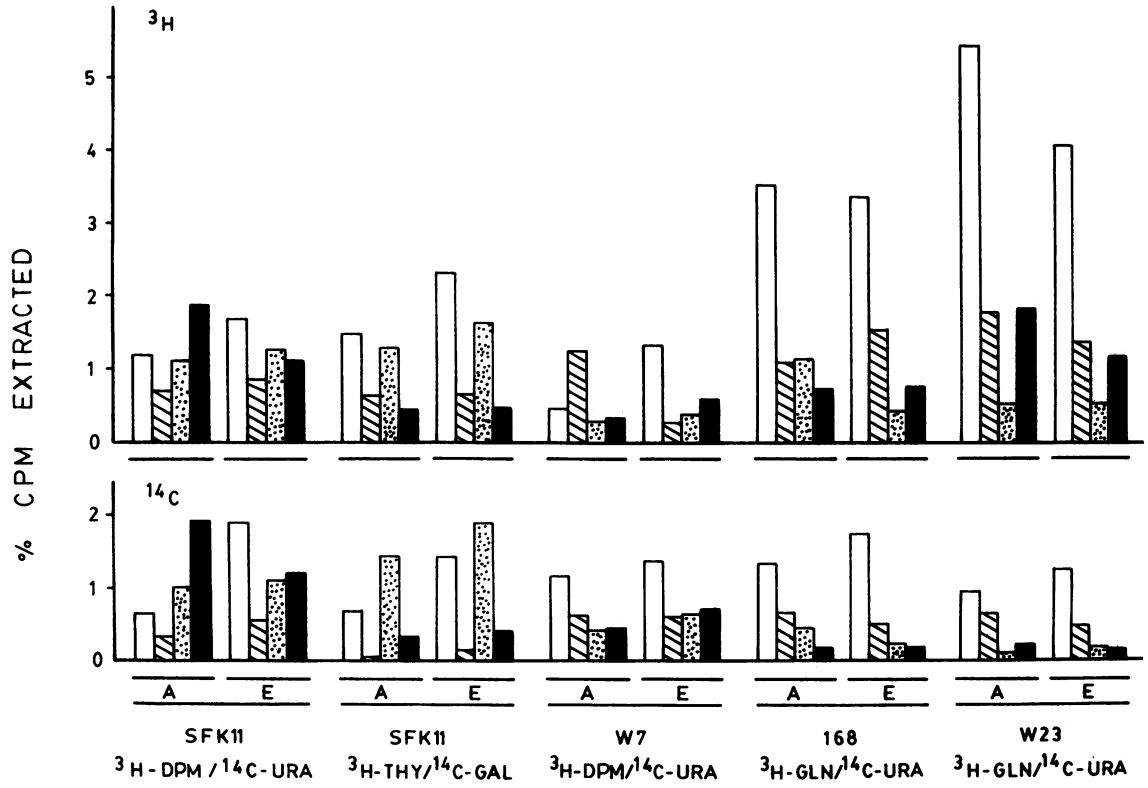

FIG. 1. Percent ^{3}H and ^{14}C cpm detected at different stages of processing during conventional embedding of *E. coli* SFK11 and W7 and *B. subtilis* 168 and W23 with either acetone (A) or ethanol (E) as the dehydrating agent. Isotopes used: DPM, diaminopimelic acid; URA, uracil; THY, thymidine; GLN, *N*-acetyl-D-glucosamine. Open bars, Dehydration stage; hatched bars, transition stage in propylene oxide; infiltration stage in either Spurr resin (stippled bars) or Epon 812 resin (solid bars).

steps to enhance infiltration of resins, it is possible to proceed directly from dehydration to infiltration when acetone is used as a dehydrating agent (9). This is an especially attractive alternative since we show that acetone is generally less deleterious for dehydration of eubacteria. Detection of radiolabels was variable for the two resins; no correlation between degree of extraction, label combination, and resin was apparent.

Radiolabel detection in cells prepared for freeze-substitution. Table 2 presents the total percent cpm detected during freeze-substitution of dual-labeled bacteria. Very little label was detected during the substitution step of processing. In subsequent stages, gram-negative and gram-positive cells behaved differently. Gram-negative cells lost the majority of labeled material during the acetone washes, and, in contrast to conventional dehydration, most of this label was released in the first of the six rinses. With each successive wash, significantly less label was recovered. Few cpm were detected in the infiltration resin of *E. coli* cells. Although a similar pattern of label loss was observed in the acetone washes of *B. subtilis*, higher isotope concentrations were recovered from the infiltrating resins, particularly the peptidoglycan label.

Autoradiography and densitometry of freeze-substituted radiolabeled bacteria. In an attempt to explain the higher levels of isotopes observed in processing solvents of freeze-substituted cells, a qualitative estimate of freezing damage was obtained. Sample wedges collected at four different stages during processing (before plunge-freezing, after freezing but before substitution, after substitution, and after

TABLE 2. Percent ^{3}H and ^{14}C cpm detected as soluble material in processing fluids during freeze-substitution of *E. coli* SFK11 and W7 and *B. subtilis* 168 and W23

Processing fluid	% of added cpm[a]									
	E. coli						*B. subtilis*			
	SFK11		SFK11		W7		168		W23	
	[^{3}H]DPM	[^{14}C]Ura	[^{3}H]Thy	[^{14}C]Gal	[^{3}H]DPM	[^{14}C]Ura	[^{3}H]GlN	[^{14}C]Ura	[^{3}H]GlN	[^{14}C]Ura
Substitution medium	<0.1	<0.1	<0.10	<0.1	3.09	0.42	2.25	0.37	0.83	0.06
Acetone washes	33.5	31.92	44.14	42.17	4.93	26.53	8.59	23.24	8.91	28.81
Infiltration resin	1.6	1.46	3.64	3.7	2.67	16.55	34.73	6.41	27.65	10.28
Total	35.1	33.38	47.77	45.87	10.69	43.5	45.57	30.02	37.39	39.15

[a] DPM, Diaminopimelic acid; Ura, uracil; Thy, thymidine; Gal, galactose; GlN, *N*-acetylglucosamine.

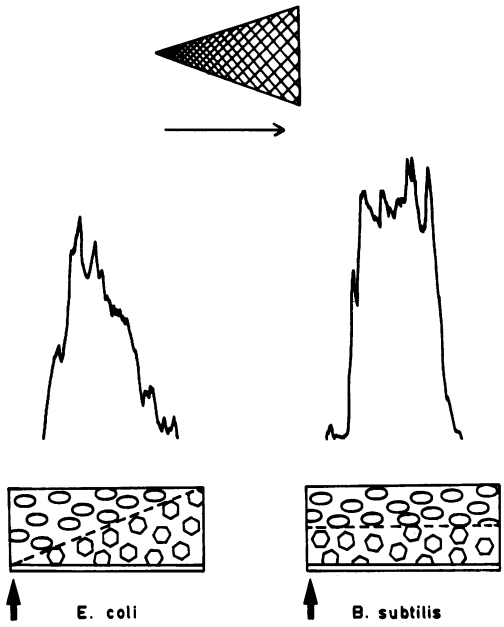

FIG. 2. Representative optical densitometry scans obtained from actual sample wedge autoradiograms of *E. coli* W7 and *B. subtilis* 168 cells. The scans presented are of sample wedges collected following substitution. Uppermost arrow indicates direction of scan across wedge. In the proposed model of freezing patterns (bottom) determined for gram-negative and gram-positive cells, the arrow at the left of each diagram indicates the initial freezing edge of sample wedges observed in cross section; ovals represent well-frozen cells, and hexagons represent freeze-damaged cells.

infiltration) were used to construct autoradiograms. The developed autoradiograms were then scanned by an optical densitometer along a linear track from the initial freezing edge (the wedge shape allows orientation of the sample so that the point is the first sample surface to contact the cryogen) to the final edge (the back of the wedge enters the cryogen last). Since peak height is correlated with grain density, greater grain density in the autoradiogram implies greater radiolabel retention in the sample. The first edge to contact the cryogen should undergo the fastest freezing and have minimal freezing damage. The point of the sample wedge which contacts the cryogen first should therefore have minimal freezing damage. Consequently, cells at this location should retain most or all of their label, and the resulting autoradiogram should express the greatest grain density in this region. If the rate of freezing deteriorates towards the rear of the sample, allowing ice crystal formation and growth, denaturation of macromolecular structure and subsequent cell lysis will result. This will be reflected in decreasing grain density of the autoradiogram.

From the shapes of the tracings, it became apparent that gram-positive and gram-negative cells were behaving differently during processing. When scanned from leading to final freezing edge, grain density was relatively consistent across autoradiograms of *B. subtilis* cells taken before and after freezing and after substitution (Fig. 2). Corresponding tracings of the gram-negative cells, however, showed a peak at the leading edge, which gradually decreased towards the final freezing edge (Fig. 2). Although the geometry of the triangular support suggests that, during freeze-plunging, cells along the border of the support should freeze at a rate equal to that of cells on the tip, data from electron microscopy and autoradiograms indicate that this is not the case. The unfrozen wedge of *E. coli* cells expressed constant grain density across its length and yielded tracings similar to those observed in wedges of *B. subtilis* cells. Although the peak area (area under the tracing) remained constant for *E. coli* cells autoradiographed before and after freezing and after both substitution and infiltration, a significant decrease was observed after infiltration of *B. subtilis* cells, implying significant label loss at this stage of processing.

Morphological detail of cells processed by both techniques. Direct electron microscopic observation of thin sections of cells processed by both techniques revealed striking differences in cell wall architecture. Representative micrographs of *E. coli* SFK11 and *B. subtilis* 168 processed by freeze-substitution and conventional embedding are presented in Fig. 3, 5, 7, and 9. A multilayered wall showing the cytoplasmic membrane, "periplasmic gel" (12), and asymmetrically staining outer membrane was very apparent in freeze-substituted *E. coli* cells (Fig. 5). Infrastructure within the gram-positive wall (Fig. 9) was also visible in the form of a dense fibrous "inner wall" and a more loosely fibrous "outer wall" extending beyond the inner wall. This fibrous layer was not observed in conventionally prepared cells (Fig. 7), nor was the electron-dense periplasmic gel of *E. coli* cells (Fig. 3). These layers become very apparent when electron density was measured by optical densitometry.

Figures 4, 6, 8, and 10 show the tracings produced from scans perpendicular to a cross section of the cell wall of *E. coli* and *B. subtilis* cells prepared by conventional and freeze-substitution methods. Conventionally prepared *B. subtilis* cell walls (Fig. 8) appeared to have condensed during processing and were electron dense and of equal thickness; gram-negative walls were wavy and of irregular width (Fig. 4). The appearance of the cytoplasm differed in cells processed by both techniques. The cytoplasm of freeze-substituted cells was granular and of even electron density and contained evenly distributed ribosomes. In contrast, that of conventionally prepared cells contained more voids, often partially filled with fibrous material. Not all of the freeze-substituted cells examined had the robust appearance described. Cells of distorted shape and those containing cytoplasmic voids (induced by ice crystal formation) were increasingly apparent nearest the support matrix (cellulose-ester filter) and in sections cut from the rear of the sample wedge (the end last to contact the cryogen), the regions most susceptible to slower freezing and thus to greatest freezing damage. No visual difference was apparent between cells dehydrated in either acetone or ethanol or infiltrated in Spurr or Epon 812 resin.

DISCUSSION

Until recently, much of the information obtained by electron microscopy concerning eubacterial ultrastructure was obtained from thin sections of conventionally prepared cells. Numerous artifacts associated with this processing method have been described and must be considered during image interpretation. Freeze-substitution is an alternative technique which should be superior to conventional methods since it combines physical fixation (ultrarapid freezing to instantaneously arrest physiological processes and freeze cellular constituents in their natural position) with gentle chemical fixation and dehydration, yielding specimens that are miscible with standard plastic resins. Since the cell is chemically stabilized while frozen in its native form, structure should be better retained in thin sections; artifacts

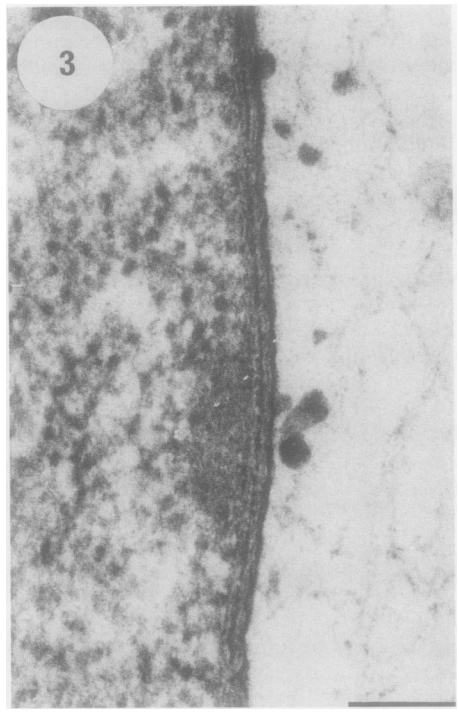

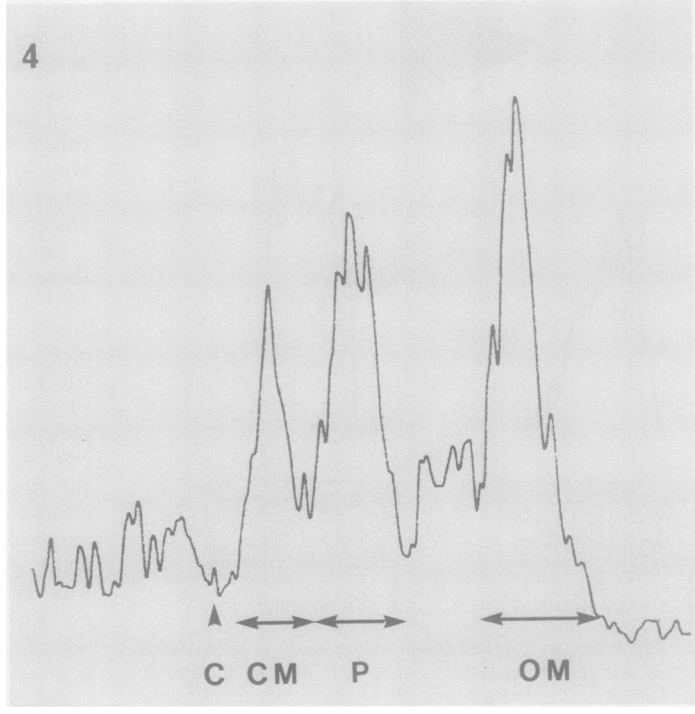

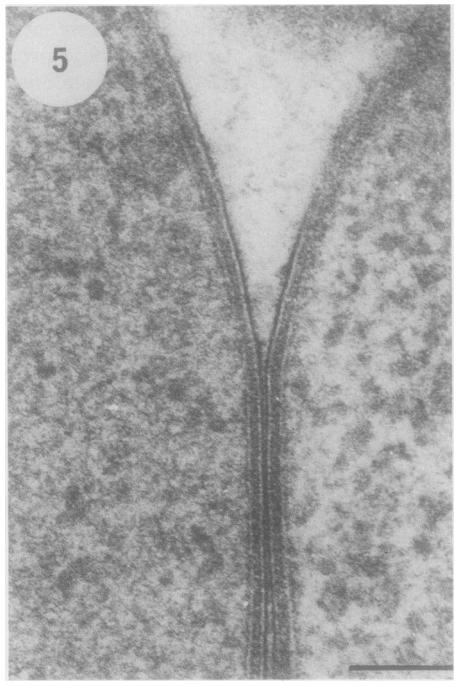

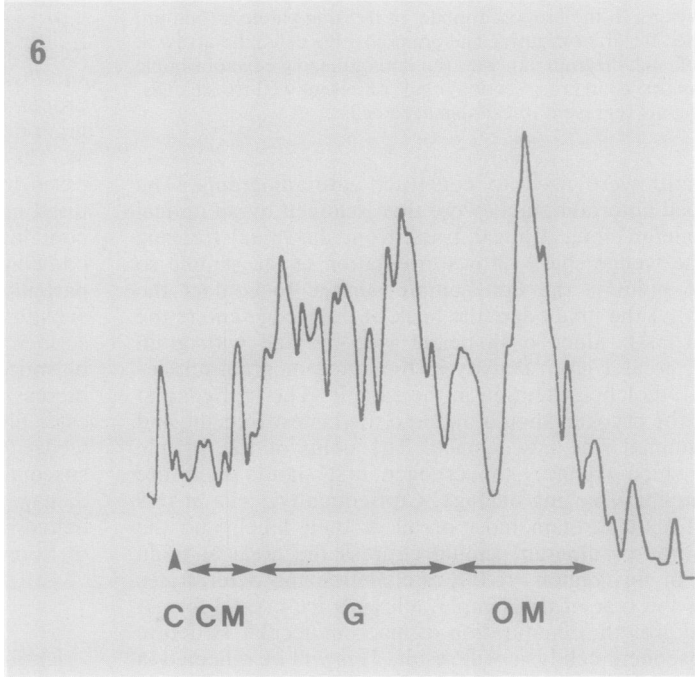

FIG. 3–6. *E. coli* envelopes.

FIG. 3. Micrograph of *E. coli* SFK11 envelope prepared by conventional embedding methods with acetone dehydration and infiltration in Epon 812. Notice that the peptidoglycan is a single electron-dense line. Bar, 100 nm.

FIG. 4. Optical densitometry scan of envelope shown in Fig. 3. OM, Outer leaflet of outer membrane; P, peptidoglycan; CM, cytoplasmic membrane; C, cytoplasm.

FIG. 5. Micrograph of *E. coli* SFK11 envelope prepared by freeze-substitution. Notice that the peptidoglycan cannot be differentiated from the periplasmic gel. Bar, 100 nm.

FIG. 6. Optical densitometry scan of envelope shown in Fig. 5. Symbols as in Fig. 4; G, periplasmic gel.

associated with conventional processes, such as cell shrinkage and collapse of cell structure (10) as well as redistribution and denaturation of molecular components (1, 7), should be minimized. Although freeze-substitution offers an alternative technique, no criteria have yet been defined to assess how representative are the resulting images of bacteria. Clearly, the ultrastructural details are different from those obtained by other processing methods, but the technique

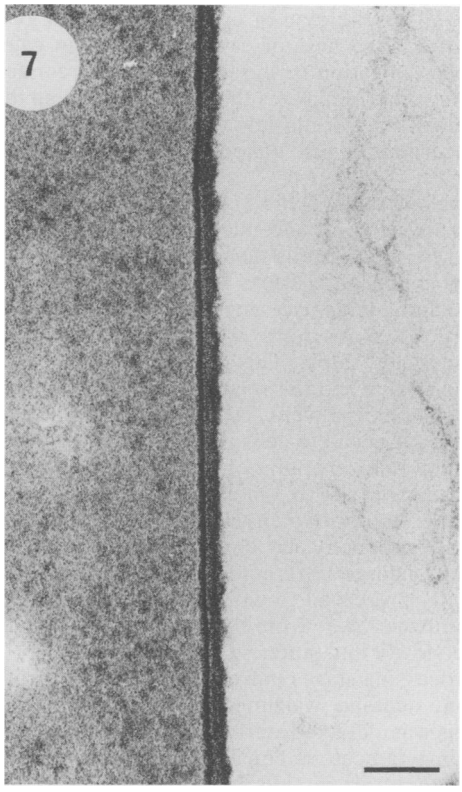

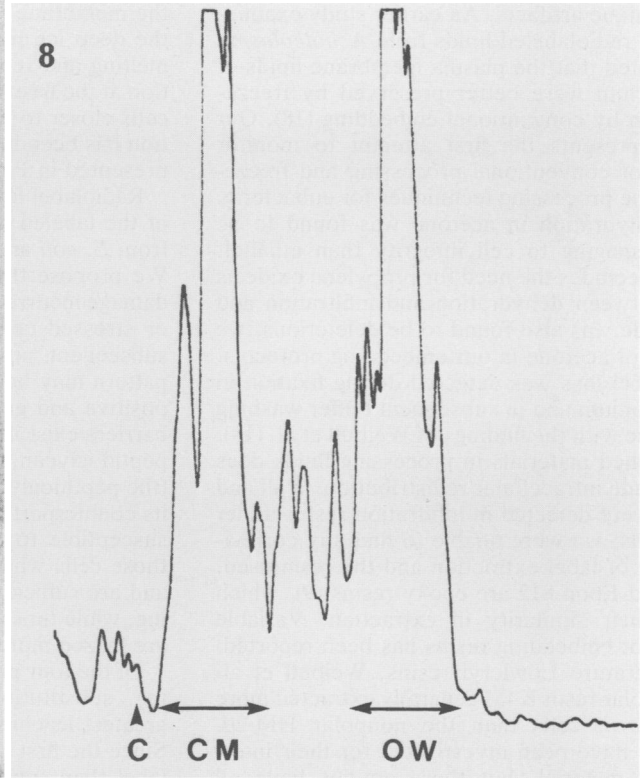

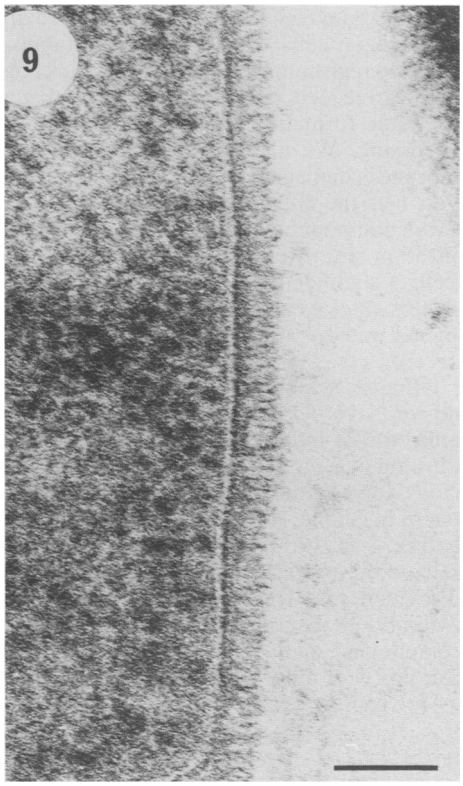

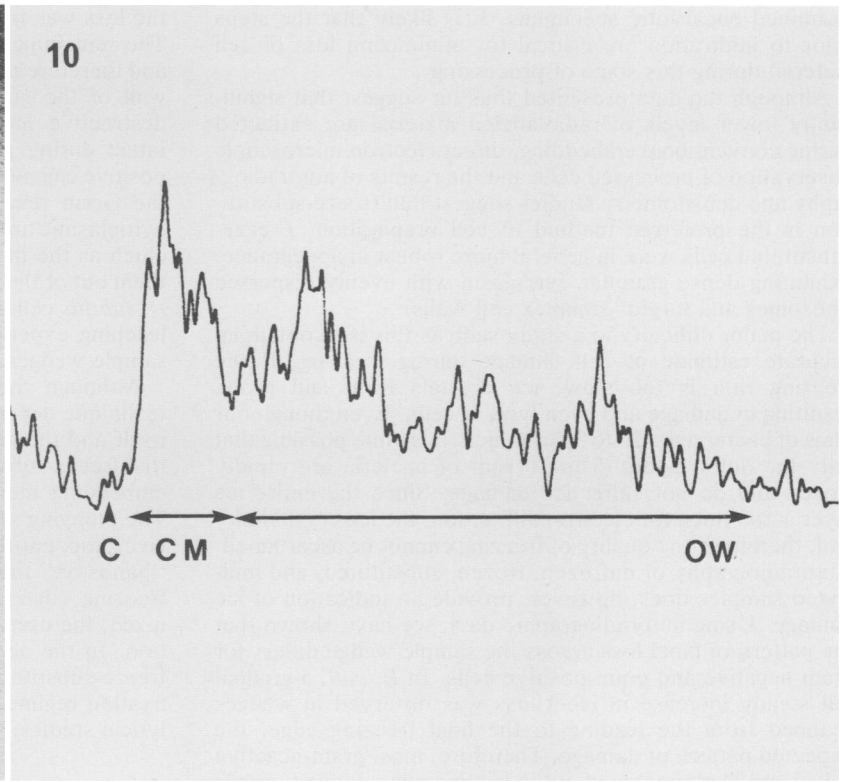

FIG. 7–10. *B. subtilis* cell wall.

FIG. 7. Micrograph of *B. subtilis* 168 cell wall prepared by conventional embedding methods with ethanol dehydration and infiltration in Epon 812. Note the condensed cell wall. Bar, 100 nm.

FIG. 8. Optical densitometry scan of the cell wall shown in Fig. 7. C, Cytoplasm; CM, cytoplasmic membrane; OW, outermost edge of cell wall.

FIG. 9. Micrograph of *B. subtilis* 168 cell wall prepared by freeze-substitution. Note the thick fibrous cell wall. Bar, 100 nm.

FIG. 10. Optical densitometry scan of the cell wall shown in Fig. 9. Labels are as in Fig. 8. Note the extent of the cell wall.

possesses its own unique artifacts. An earlier study examining the extraction of radiolabeled lipids from *Acholeplasma laidlawii* cells indicated that the plasma membrane lipids of this wall-less bacterium were better preserved by freeze-substitution (19) than by conventional embedding (18). Our study, however, represents the first attempt to monitor directly the effects of conventional processing and freeze-substitution as routine processing techniques for eubacteria.

In our hands, dehydration in acetone was found to be significantly less damaging to cell integrity than ethanol. Since this solvent precludes the need for propylene oxide as a transition fluid between dehydration and infiltration and since propylene oxide was also found to be deleterious, we recommend the use of acetone in our embedding protocols.

That little radiolabel loss was detected during fixation in glutaraldehyde or osmium and in subsequent buffer washing steps is in accordance with the findings of Weibull et al. (18). The absence of leached materials in processing fluids does not, however, preclude intracellular redistribution. Wall and nucleic acid labels were detected in infiltration resins under all labeling conditions; we were unable to find any correlation between degree of label extraction and the resin used. Both Spurr resin and Epon 812 are epoxy resins (9), which may account for their similarity in extraction. Variable extraction in different embedding resins has been reported. With the low-temperature Lowicryl resins, Weibull et al. (18) found that the polar resin K4M generally extracted more lipid from *A. laidlawii* cells than the nonpolar HM-20. Several other resins have been investigated for their interaction with sample material, but these studies have all examined eucaryotic specimens. It is likely that the steps prior to infiltration are critical for minimizing loss of cell material during this stage of processing.

Although the data presented thus far suggest that significantly lower levels of radiolabeled material are extracted during conventional embedding, direct electron microscopic observation of processed cells and the results of autoradiography and densitometry studies suggest that freeze-substitution is the preferred method of cell preparation. Freeze-substituted cells were in general more robust in appearance, exhibiting dense granular cytoplasm with evenly dispersed ribosomes and turgid, complex cell walls.

The major difficulty in a study such as this is to obtain an accurate estimate of cell damage during freezing. If the freezing rate is too slow, ice crystals form and grow, resulting in damage and even lysis of cells. Even though our films of bacteria are 20 to 30 μm thick, it is quite possible that only the outer layers (5 to 10 μm) of bacteria are rapidly frozen and do not suffer ice damage. Since the entire ice layer is too thick for electron diffraction, the ice crystallinity and, therefore, the quality of freezing cannot be ascertained. Autoradiography of unfrozen, frozen, substituted, and infiltrated samples does, however, provide an indication of ice damage. Using autoradiographic data, we have shown that the pattern of label loss across the sample wedge differs for gram-negative and gram-positive cells. In *E. coli*, a gradual but steady increase in label loss was observed in wedges scanned from the leading to the final freezing edge, the expected pattern of damage. Therefore, most gram-negative cells were best preserved at the leading edge, while towards the rear virtually all were damaged. *B. subtilis* cells, however, expressed constant grain density (and presumed constant level of ice damage) across the entire length of the sample wedges. Electron microscopic observation showed that *Bacillus* cells nearest the support membrane were the most damaged, presumably due to the insulating nature of the membrane and slow release of crystallization energy in the deep ice matrix. The heat of crystallization can cause melting and recrystallization in this region. Better conduction at the freezing edge minimizes this phenomenon, so that cells closer to the surface suffer less damage. This information has been incorporated into a model of freezing which is presented in Fig. 2.

Radiolabel leaching data (Table 2) suggest that up to 50% of the labeled material (wall and nucleic acid) may be lost from *E. coli* and *B. subtilis* cells during freeze-substitution. We propose that much of this loss is induced by freezing damage incurred at the initial freezing step. Freeze-damaged or stressed cells would be more prone to leakage during subsequent processing steps. This difference in freezing pattern may be attributed to the relative strengths of gram-positive and gram-negative walls. Although three potential barriers exist in gram-negative cells (the plasma membrane, peptidoglycan, and outer membrane), each is relatively thin (the peptidoglycan layer is 1 to 3 molecules thick relative to its counterpart in gram-positive envelopes) and is thus more susceptible to disruption by ice damage. Therefore, only those cells which undergo ultrarapid freezing remain intact and are sufficiently preserved to withstand further processing, while those further away from the leading freezing edge are frozen more slowly and suffer severe ice damage.

Of the four processing stages in freeze-substitution (freezing, substitution, acetone washing, and infiltration), the greatest leaching was detected during the acetone washes. Since the first rinse in acetone consistently contained more label than subsequent processing fluids, this suggests that the loss was from cells damaged during the initial freezing. The remaining well-frozen cells were adequately stabilized and therefore relatively resistant to leaching. The thick, rigid wall of the gram-positive cell is better able to withstand destructive ice crystal formation and therefore remains intact during processing. We also suggest that the gram-positive cell membrane is damaged during freezing, but, as in the Gram reaction (2), the thick fibrous cell wall retains cytoplasmic and wall components until a viscous component (such as the infiltration resin) remobilizes them and carries them out of the cell. A significant loss of peptidoglycan from *B. subtilis* cells at this stage of processing was noted both in leaching experiments and by autoradiographic analyses of sample wedges.

Although the ultimate selection of sample preparation technique depends on several criteria, including the sample itself and the nature of the information desired, we believe that freeze-substitution is a good alternative to conventional embedding methods for routine processing of eubacteria. The plunging system is simple, it can be relatively inexpensive, the entire freeze-substitution process requires less "hands-on" time, and the bacteria are well preserved at the freezing edge. Provided that freezing artifacts are recognized, the user will obtain accurate ultrastructural information. In the accompanying manuscript (8), we explore the freeze-substitution protocol more fully and suggest optimal fixation regimens for routine processing and for microanalytical studies.

ACKNOWLEDGMENTS

We gratefully acknowledge Tom Irving, Department of Physics, University of Guelph, for help with the optical densitometry.

This research was supported by a Medical Research Council of Canada operating grant to T.J.B. The microscopy was performed in the NSERC Guelph Regional STEM Facility, which is maintained by funds from the Department of Microbiology, the College of

Biological Sciences, and the Natural Sciences and Engineering Research Council of Canada.

LITERATURE CITED

1. **Aldrich, H. C., D. B. Beimborn, and P. Schonheit.** 1987. Creation of artifactual internal membranes during fixation of *Methanobacterium thermoautotrophicum*. Can. J. Microbiol. **33:** 844–849.
2. **Beveridge, T. J., and J. A. Davies.** 1983. Cellular responses of *Bacillus subtilis* and *Escherichia coli* to the Gram stain. J. Bacteriol. **156:**846–858.
3. **Beveridge, T. J., and S. F. Koval.** 1981. Binding of metals to cell envelopes of *Escherichia coli* K-12. Appl. Environ. Microbiol. **42:**325–335.
4. **Coetzee, J., and C. F. van der Merwe.** 1989. Extraction of carbon 14-labeled compounds from plant tissue during processing for electron microscopy. J. Electron Microsc. Techniques **11:**155–160.
5. **Cope, G. H., and M. A. Williams.** 1969. Quantitative studies on the preservation of choline and ethanolamine phosphatides during tissue preparation for electron microscopy. I. Glutaraldehyde, osmium tetroxide, araldite methods. J. Microsc. **90:** 31–46.
6. **Cope, G. H., and M. A. Williams.** 1969. Quantitative studies on the preservation of choline and ethanolamine phosphatides during tissue preparation for electron microscopy. II. Other preparatory methods. J. Microsc. **90:**47–60.
7. **Ebersold, H. R., J.-L. Cordier, and P. Luthy.** 1981. Bacterial mesosomes: method-dependent artifacts. Arch. Microbiol. **130:** 19–22.
8. **Graham, L. L., and T. J. Beveridge.** 1990. Effect of chemical fixatives on accurate preservation of *Escherichia coli* and *Bacillus subtilis* structure in cells prepared by freeze-substitution. J. Bacteriol. **172:**2150–2159.
9. **Hayat, M. A.** 1986. Basic techniques for transmission electron microscopy. Academic Press, Inc., New York.
10. **Hayat, M. A.** 1981. Fixation for electron microscopy. Academic Press, Inc., New York.
11. **Hobot, J. A., E. Carleman, W. Villiger, and E. Kellenberger.** 1984. Periplasmic gel: new concept resulting from the reinvestigation of bacterial cell envelope ultrastructure by new methods. J. Bacteriol. **160:**143–152.
12. **Hobot, J. A., W. Villiger, J. Escaig, M. Maeder, A. Ryter, and E. Kellenberger.** 1985. Shape and fine structure of nucleoids observed on sections of ultrarapidly frozen and cryosubstituted bacteria. J. Bacteriol. **162:**960–971.
13. **Mobley, H. L. T., R. J. Doyle, U. N. Streips, and S. O. Langemeier.** 1982. Transport and incorporation of *N*-acetyl-D-glucosamine in *Bacillus subtilis*. J. Bacteriol. **150:**8–15.
14. **Reynolds, E. S.** 1963. Use of lead citrate as a stain in electron microscopy. Cell Biol. **17:**208–213.
15. **Silva, M. T., and J. C. F. Sousa.** 1973. Ultrastructure of the cell wall and cytoplasmic membrane of gram-negative bacteria with different fixation techniques. J. Bacteriol. **113:**953–962.
16. **Spizizen, J.** 1958. Transformation of biochemically deficient strains of *Bacillus subtilis* by deoxyribonucleate. Proc. Natl. Acad. Sci. USA **44:**1072–1078.
17. **Weibull, C. W., and A. Christiansson.** 1986. Extraction of proteins and membrane lipids during low temperature embedding of biological material for electron microscopy. J. Microsc. **142:**79–86.
18. **Weibull, C., A. Christiansson, and E. Carlemalm.** 1983. Extraction of membrane lipids during fixation, dehydration and embedding of *Acholeplasma laidlawii* cells for electron microscopy. J. Microsc. **129:**201–207.
19. **Weibull, C., W. Villiger, and E. Carlemalm.** 1984. Extraction of lipids during freeze-substitution of *Acholeplasma laidlawii* cells for electron microscopy. J. Microsc. **134:**213–216.